Bulletin of Earthquake Engineering (2022) 20:1739–1765
https://doi.org/10.1007/s10518-021-01280-0

ORIGINAL ARTICLE

Seismic response of a small-scale masonry groin vault: experimental investigation by performing quasi-static and shake table tests

N. Bianchini[1] · N. Mendes[1] · C. Calderini[3] · P. X. Candeias[2] · M. Rossi[4] · P. B. Lourenço[1]

Received: 21 January 2021 / Accepted: 7 November 2021 / Published online: 21 January 2022
© The Author(s), under exclusive licence to Springer Nature B.V. 2021

Abstract
The seismic safety assessment of 3D complex structural elements of historic buildings, such as groin and rib vaults, is a challenge and experimental tests can provide relevant data for this purpose. This paper presents the results of two experimental campaigns about a reduced scale 3D printed vault characterized by asymmetric boundary conditions. The specimen adopted the square plan geometry of groin vault and was made of polymeric bricks with radial joints, orthogonally woven at the barrel intersection. The seismic behaviour of the vault was studied through physical modelling: quasi-static using actuators and dynamic using a shake-table. In particular, an incremental dynamic analysis up to the collapse of the vault was carried out. The results obtained experimentally were analysed in terms of damage, collapse mechanisms, ultimate displacements, and response spectrum-based analysis.

Keywords Groin vault · Displacement-based assessment · Experimental tests · Quasi-static tests · Seismic response · Shake table tests

1 Introduction

Masonry cross vaults represent one of the most important structural typologies within European cultural heritage buildings. Mostly developed during the Roman Empire and in the period between the High Middle Ages and Renaissance until nowadays, groin and rib vaults reached a level of beauty and construction technique that still amazes the modern observer. For centuries, experiences and instructions had been secretly transmitted between ancient masons as rules of thumb, which have guaranteed their long-lasting history (Gaetani et al. 2016). However, being conceived to withstand only gravitational loads, masonry vaults are threatened by seismic events (Doglioni, Moretti, and Petrini 1994; Regione Toscana 2003; National Civil Protection Service 2013; Podestà et al. 2010).

✉ N. Bianchini
nicoletta.bianchini@gmail.com
http://www.isise.net

Extended author information available on the last page of the article

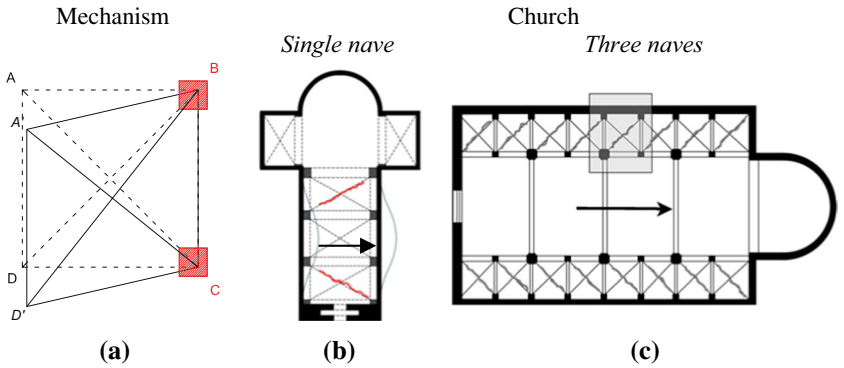


Fig. 1 **a** In-plane shear displacement settings considered in the experimental campaign (Rossi et al. 2016). **b** Single-nave mechanism **c** Three-naves mechanism

In this regard, considering the limited research in the field, the present paper aims at investigating the seismic behaviour of masonry groin vaults subjected to shear displacement of the abutments (Fig. 1). The need of this research is due to the fact that, in most cases, the groin vaults are capable of sustaining significantly larger vertical displacements than horizontal displacements before collapse occurs (Mcinerney and Dejong 2015). This particular type of cross vault (groin vault) is theoretically the geometrical result of the intersection at a right angle of two semi-circular barrel vaults, characterised by the lack of diagonal ribs. Groin vaults are very often used in the covering of churches' naves, palaces' rooms, and porticos, especially in the Italian territory. Thus, the present research work has three main aims:

- Evaluation of the damage and collapse mechanism of the tested specimen under different loading conditions;
- Depiction of the resistance to shear displacement of the abutments, under quasi-static and dynamic actions, analysing the same test specimen;
- Studying the influence of the frequency content of the ground-motion on the same test specimen, considering a registered past Italian earthquake and one expected by the Italian code;

The first aim is to evaluate the three-dimensional damage and collapse mechanism of masonry groin vaults subjected to horizontal shear forces caused by the seismic action. In-plane shear behaviour is a common type of failure that occurs during an earthquake as it was widely observed during post-earthquake surveys (Arcidiacono et al. 2016; Carfagnini et al. 2018; Borri et al. 2002).

The second aim of this research work is to investigate the shear capacity of groin vaults in terms of forces and displacement, using two different experimental approaches. The first approach is static and corresponds to the quasi-static tests performed by Rossi et al. (2015) at the University of Genoa, where monotonic horizontal displacements were applied at the abutments. The second approach is dynamic and is based on an extensive shake table tests campaign performed in the National Laboratory for Civil Engineering, Lisbon, Portugal (LNEC) within the context of the project "Seismology and Earthquake Engineering Research Infrastructure Alliance for Europe" (SERA). The crucial point of this research

is that the same test specimen, a reduced scale (1:5) groin vault made of 3D printed polymeric blocks, has been used in the two approaches. Experiments where a same test specimen is used for both quasi-static and dynamic testing are rare. For example, Calderini et al. (2015)studied both statically and dynamically a scaled arch-pier system reinforced with tie-rods, but no curved structures such as vaults were studied through both static and dynamic campaigns. The main results of Calderini et al. (2015) showed that, in general, the force and displacement capacity of the tested model is lower than the ones predicted by theoretical analysis; this may be attributed to the deformability of the system in both the elastic and inelastic range and the presence of imperfections in the contacts between blocks. On the other hand, shake table tests proved the importance of considering displacement capacity for the seismic assessment of ancient masonry structures and, even more, in the design of strengthening techniques. From these considerations, it was possible to compare in terms of displacements the two approaches, using the response spectra for a Single-Degree-Of-Freedom (SDOF) to assess the performance of the structure based on linear kinematic analysis (Cattari et al. 2008; Lagomarsino and Resemini 2009; D'Ayala 2005; D'Ayala and Tomasoni 2011; Mousavian and Casapulla 2020). Even if such study led to important conclusions, the results are only valid for a 2D structure. The research presented in this paper aims at extending the study to a three-dimensional behaviour. The comparison between static and shake table tests is fundamental because, in the most recent codes and guidelines, nonlinear static analysis is still the most used type of analysis to assess the behaviour of the masonry structures (static approach) (Modena 2020; Bianchini et al. 2019). Still, nonlinear dynamic analysis, despite the heavier computational effort, may lead to more realistic results.

Finally, the third aim of this research work is related to the influence of two different types of ground motion on the performance of the test specimen. Namely, the recorded ground motion which hit Emilia region (Italy) in 2012, and an artificial accelerogram based on the code spectrum were selected. This is a region where many monumental buildings present groin vaults as proved by post-earthquake damage and surveys.

1.1 Shear failure investigation

Historically, groin and rib vaults showed advantages which made them more desirable than other vaults. Advantages include the structural stability, the simplicity, and the flexibility to provide natural light to the interior places, and the aesthetics. At the same time, a groin or a rib vault requires less quantity of material, compared to other kinds of vaults (*e.g.* about half of the material of a barrel vault or two-thirds less material than a pavilion vault) and it is likely one of the most visually appealing horizontal elements that allow transferring gravitational loading to piers in monumental buildings (Huerta 2004; Cangi 2012).

Despite the favourable behaviour of cross vaults under vertical static loads, the in-plane horizontal shear distortion is a damage mechanism recurrently observed during post-earthquake surveys. This kind of mechanism is rather unexplored, even if it is particularly common in single-nave churches (Fig. 1b) characterised by a large difference in stiffness between the nave and the façade and/or transept, and in three-nave churches characterised by a large difference in stiffness between the lateral wall and the colonnade (Fig. 1c) (Rossi et al. 2015; Milani et al. 2016; De Matteis et al. 2019). For this research, Fig. 1c represents the chosen condition.

In rather common cases, the lower stiffness of the central nave's colonnade, compared to the external walls, can lead to differential displacements along the longitudinal direction

and, consequently, to the development of shear damage in the horizontal structural elements. This failure is mainly identified by diagonal cracks and the test specimen used in the experimental campaign was designed to reproduce this failure using appropriate geometrical details and boundary conditions.

1.2 Experimental campaigns on masonry cross vaults

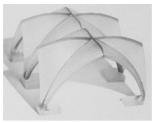
Despite the fact that the present topic interests a significant amount of real cases across the world, only a few researchers worked on masonry cross vaults (groin and ribbed ones). Bertolesi et al. (2019) provided an overview about the academic interest on this topic, highlighting that less than 40 scientific papers deal with masonry cross vaults in the period from 1960 to 2018. Moreover, in the last four years, they account for less than 1% of all the documents dealing with historic masonry structures, as found by the authors of this paper. In addition, very few researchers dealt with full experimental campaigns on shear behaviour. Table 1 summarises experimental studies developed using different materials and types of tests. Tests with specimens built at reduced scale represent an interesting approach to study the structural behaviour of masonry cross vaults, mainly the collapse mechanism, and, consequently, have been recurrently used.

Mark and O'Neill (1973) presented the first experimental study on the subject, pointing out that the major in-plane vault forces are directed to its supports, validating ancient treatises and semi-empirical rules like the ones from Abraham (1934). Among other examples, Bati et al. (2002) carried out a complete study in which different load conditions, symmetric and asymmetric boundary conditions, and strengthening techniques (mainly ties and Glass Fibre Reinforced Polymer externally bonded reinforcement) were evaluated. Theodossopoulos et al. (2002, 2003) applied an increasing horizontal displacement at the abutments up to failure, and highlighting the importance of the stability of the supporting piers and the abutments. This study has been crucial for the definition of the setup of this research, since it stressed the fact that, under service loads, the groin vault showed a high reserve in strength, developing an asymmetric deformation pattern. Such behaviour is due to the difference between the stiffness of the wall and the nave arch. Williams et al. (2012) applied a unidirectional horizontal base shaking to a reduced scale model, representing the first shake table tests performed on a cross vault. Foti et al. (2015, 2018) introduced the important aspect of the masonry bond (or unit arrangement) of the vault. They studied parallel and radial masonry bond from the experimental point of view, keeping the same geometry and material of the test specimen. Moreover, they applied displacement control tests, namely in the vertical, horizontal, and diagonal directions. In the case of diagonal failure, the experimental laboratory model showed a premature collapse due to the presence of local hinges at some edge blocks' location.

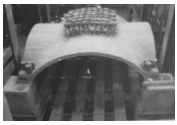
The specimen tested by Rossi et al. (2020) consists of the first shake table test performed on a 1:1 scale model. Even though the target failure mechanism was the one related to the shear failure, the vault collapsed at 0.4 g, due to the activation of an out-of-plane mechanism that led to the development of the typical four-hinge mechanism. Carfagnini et al. (2018) and Baraccani et al. (2020) performed also important works on this topic. They tested a 1:4 scaled specimen of a Gothic cross vault, subjected to shear deformation at two of its springings. It was shown that the initiation of cracks appeared perpendicularly to the diagonal ribs. It was also identified that the failure occurs at about 2.7% of the longitudinal span.

Table 1 Experimental works carried out in masonry vaults, from the 1970s until the most recent works

References	Scale	Dimensions	Type of action	Type of tests	Material
Mark et al. (1973)	1:50	0.1×0.2 m^2	Static	Dead load (Photoelastic technique)	Epoxy resin
Ceradini (1996)	1:1	9.6×10.6 m^2	Quasi-static	Vertical settlement of the supports	Bricks
Faccio et al. (1999)	1:1	7.36×7.36 m^2	Quasi-static	Monotonic point load at the key of the vault	Bricks
Bati et al.(2002)	1:3	2.3×2.3 m^2	Quasi-static	Monotonic point load at the key of the vault	Bricks 0.5 cm lime joints
Theodossopoulos et al. (2002, 2003)	1:4	1.5×1.84 m^2	Quasi-static	Horizontal displacement	Wood
Miltiadou-Fezans (2008)		1.275×0.945 m^2	Dynamic	Shaking table tests (Athens earthquake)	Bricks
Williams et al. (2012)	1:25	0.89×0.896 m^2	Dynamic	Shaking table tests (sinusoidal pulse)	Plaster and sand
De Matteis and Mazzolani (2012)	1:5.5	$\sim 2.0 \times 1.1$ m^2	Dynamic	Shaking table tests (Calitri earthquake)	Bricks
Shapiro (2012)	~1:10	278×278 mm^2	Quasi-static	Monotonic point load Spreading supports Tilting tests	Plaster and powder material
Rossi et al. (2016), Milani et al. (2016)	1:5	0.65×0.65 m^2	Quasi-static	Horizontal shear displacement Tilting plane tests	Plastic powder sintering Steel
Rossi et al. (2020)	1:1	3.50×3.60 m^2	Dynamic	Shaking table tests (Keddara earthquake)	Bricks
Fagone et al. (2016)	1:5	1.63×1.58 m^2	Quasi cyclic tests	Constant vertical load and cyclic horizontal load	Sandstone Cement lime mortar
Rossi et al. (2017b)	1:10	343×343 mm^2	Quasi-static	Monotonic pointed loads Vertical displacements of the abutments	Plaster and powder material
Cardagnini et al. (2018), Baraccani et al. (2020)	1:4	0.88×1.1 m^2	Q uasi-static	Horizontal shear displacements	Timber bricks lime mortar
Foti et al.(2015, 2018)	1:5	1×1 m^2	Quasi-static	Vertical and horizontal displacements at one support	Polystyrene
Torres et al. (2019a, b)	1:1	4×4 m^2	Quasi-static	Vertical displacements at one support	(timbrel) Bricks

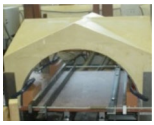

Mark et al. (1973)


Faccio et al. (1999)


Bati et al (2002)


Theodossopoulos et al. (2002; 2003)


Miltiadou-Fezans (2008)





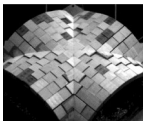
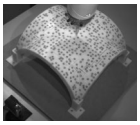






Table 1 (continued)

References	Scale Dimensions	Type of action	Type of tests	Material
Williams et al. (2012)	De Matteis and Mazzolani (2012)	Shapiro (2012)	Foti et al. (2015, 2018)	Rossi et al. (2016); Milani et al. (2016)
				
Fagone et al. (2016)	Rossi et al. (2017b)	Rossi et al. (2020; 2020)	Carfagnini et al. (2018) Baraccani et al. (2020)	Torres et al. (2019a, b)

Still, the previous studies have different assumptions and limitations. Vaults are complex structural elements, characterised by three-dimensional behaviour and connected to different types of boundary conditions. Therefore, the originality of this research is that it aims at contributing to overcome some limitations of the previous studies, reproducing a well-defined boundary condition setup to study the shear collapse, and comparing the outputs obtained by a quasi-static investigation and by a shake table test, using the same reduced-scale test specimen.

2 Description of the test specimen and test setups

2.1 Geometry and materials

The test specimen is composed of 3D printed plastic blocks with dry joints made at 1:5 scale. The shape and the geometry were defined by considering standard rules of thumb (Heyman 1995; Cangi 2009; Gaetani et al. 2015; Croci 2000; Huerta 2004) and a generic cross-section of a central bay located in a lateral nave of a three-nave church, derived from the intersection of two semi-circular barrel vaults with low rise. It is representative of a generic monumental church (Fig. 1) in Central Italy, generated by a squared base groin vault with a net span of 3.125 m and 1.125 m rise at full scale. Figure 2 presents the geometry of the test specimen.

In historical applications, it is common to find filling material placed above the corners of the vaults, which helps to reduce the thrust forces applied in the lateral piers, stabilising the thrust line (Huerta 2004). In fact, according to Heyman (1969), the safety geometric coefficient of the arch (or of the vault) is obtained by dividing the weight of the element by its thickness, which increases close to the abutments where the section of the vault intersects the filling. In this case, due to the peculiar setup, characterized by tiny dimensions and particular boundary conditions, the filling material above the corners of the vault was not considered. For the application of the filling material, more complex boundary conditions would be needed.

Thus, the test specimen is composed of 1132 blocks (Fig. 3), being 232 made fully of plastic and 880 made of plastic with a steel core (Fig. 4). They have been 3D printed with the SLS (Selective Laser Sintering) technology, which allows to generate small-scale models by a numerically controlled machine starting from a 3D digital model, with high

geometrical accuracy (±0.1 mm) and a reasonably short time of production. Indeed, the time of production was estimated between 4–5 h for the blocks of the shell, and 2 h for the supports, counting a total duration of about 6–7 h.

The adopted plastic material is a composite of zp150 powder and zb61 clear binder, printed with a ZPrinter 650. After production, the blocks have been impregnated with Z-bond 101 for improving the strength and durability. This technique was previously adopted by Rossi et al. (2017a) and ensures good stiffness and friction to take into account rigid block assumption, to allow the repeatability of the tests by minimizing the damage. Indeed, the choice of adopting this particular material and technology was led by the need of performing several tests with different configurations without causing damage to the units.

The standard blocks (red blocks in Fig. 3a) were designed, by scaling per 5 the typical dimensions of clay bricks, namely $0.06 \times 0.12 \times 0.24$ m^3 (respectively width, thickness, and length), aiming at simulating the most common bond stereotomy of groin vaults in Italy. Width and thickness dimensions are fixed at the values of 12 and 24 mm, while blocks with different lengths are placed along the outer edges of the webs to guarantee the offset of the joints, which was set ¼ of the length of the longest unit (Fig. 3a). Each block was identified by a numeric code, in order to easily rebuild the test specimen after each test. The blocks are arranged radially. Their shape is slightly trapezoidal to compensate for the absence of mortar between them (Fig. 4a) and special care was taken to design the stereotomy of the elements located along the diagonals (grey blocks in Fig. 4b) to guarantee the correct interlocking between adjacent webs. The geometry of the vault, the choice of the radial orientation, and the definition of the cuts along the diagonals were based on the rules of thumb reported by Rodrigo Gil de Hontañón (cited in Sanabria 1982), Formenti (1893), Heyman (1982), Heyman (1995), Huerta (Huerta 2004), Cangi (2012), Como (2013), Giovanetti (2000).

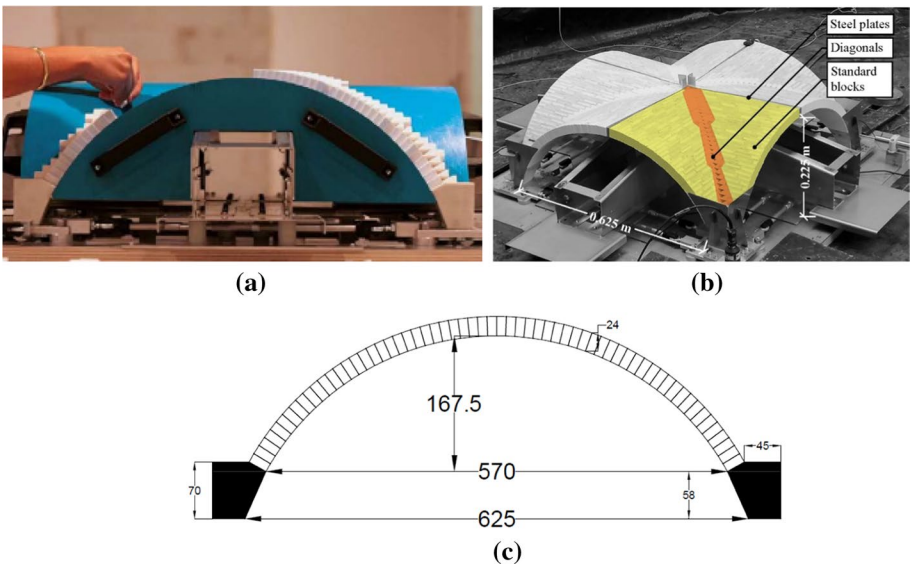


Fig. 2 Reduced scale vault: **a** details of the construction on the plywood scaffolding and **b** at the end of the construction; **c** main dimensions of the test specimen in mm

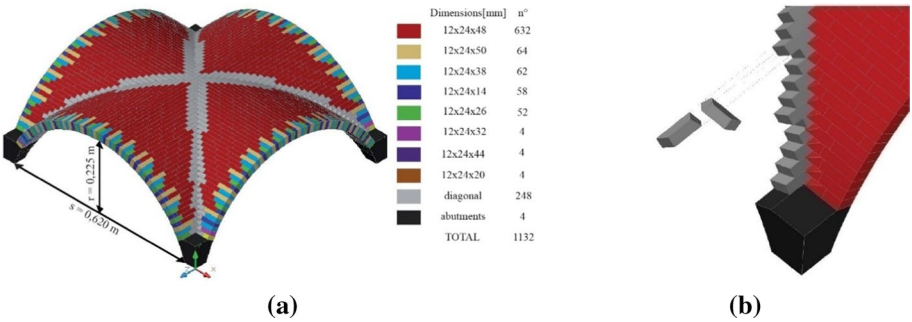


Fig. 3 Geometry of the reduced-scale vault and blocks stereotomy of the diagonal blocks (Rossi et al. 2016)

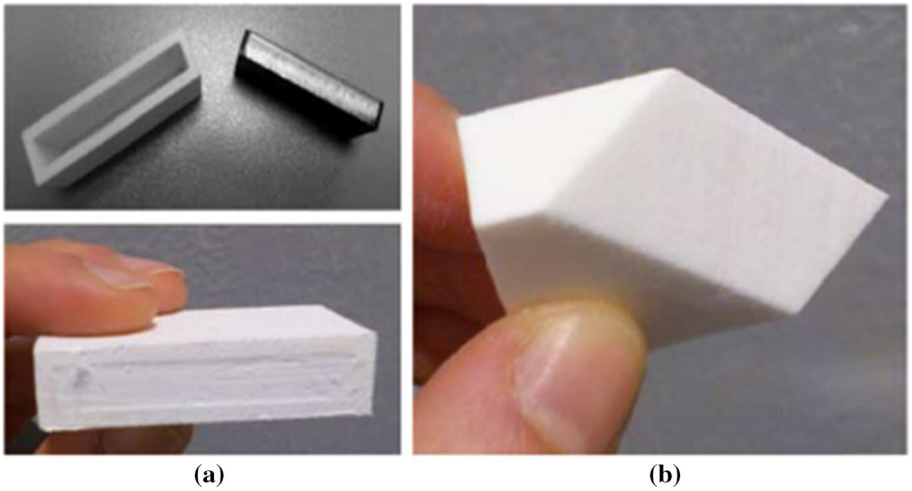


Fig. 4 Details of the standard blocks with steel core (**a**) and the elements of the diagonals (**b**)

This masonry bond needs a temporary structure for the construction of the shells. Therefore, a scaffolding made of plywood has been designed, which is composed of four pieces corresponding to the vault webs. Once the test specimen is built, the scaffolding is removed by letting the pieces slide on proper inclined rails. Care and attention are required to remove the scaffolding, in order not to incur into undesirable configurations and defects. This aspect is important to ensure the repeatability of the tests, since defects in the construction process could compromise the analysis of the results and their comparisons.

The material density (ρ) of the composite of zp150 powder and zb61 clear binder was determined to be equal to 0.55 ± 0.02 g/cm^3. Since it corresponds to a low-density value, the weight of the standard blocks and the blocks along the outer edges was increased by inserting a steel core inside each block (Fig. 4a). This was done to increase the axial compressive stress of the shell of the vault, improving its stability.

In this way, the density of the standard blocks (yellow blocks in Fig. 2b) was measured at the value of 2.70 ± 0.05 g/cm3. This strategy was not possible to be performed for the

blocks of the diagonals (orange blocks in Fig. 2b), because of their irregular shape and tiny volume which could not host a steel plate inside, as shown in Fig. 4b. Thus, the disposition of the densities along the test specimen follows the scheme already introduced in Fig. 2b, where standard blocks (in yellow) and diagonals (in orange) are associated to $\rho = 2.70$ g/cm^3 and $\rho = 0.55$ g/cm^3, respectively, for all the four symmetric webs. Both densities were measured with an electronic scale loaded with several blocks.

The final weight of the test specimen is about 35.6 kg, while the whole structure is about 43 kg, considering the steel base at the bottom of the test specimen. The friction angle (μ) of the blocks is estimated equal to $29.6° \pm 2.46°$, determined by testing 12 samples of standard blocks on the tilting table. Due to the accumulation of error in the 3D printing of the blocks, very thin steel plates ($\rho = 7.8$ g/cm^3, $E = 210{,}000$ MPa) have been properly designed and placed at the key of the vault to perfectly close its shell (Fig. 2b). Their thickness varies from 3 mm (at the outer edges) to < 1 mm (at the centre of the vault), while their length is fixed (48 mm).

Although the test specimen presents different types of materials and the scale reduction factor equal to 5 is considerable, the test specimen is still able to represent the main features of masonry groin vaults. As referred by ancient treatises (Heyman 1995), masonry cross vault's behaviour is mainly linked to the geometry of the system, namely size and shape, less depending on mechanical properties. The scale is less important for static tests (unless of important nonlinear geometric effects, such as in shallow arches or vaults), but it is much relevant for dynamic tests, as highlighted by the work of De Lorenzis et al. (2007).

The choice of using a dry joint test specimen is also an important aspect. Dry joints models may represent not only real dry joint masonry structures, but also ancient mortar joint structures whose mortared joints suffered decay during the time, decreasing their already low tensile strength (Lourenço and Ramos 2004; Pulatsu et al. 2019). A dry joint test specimen also allows to easily perform several tests, without changing the initial conditions. Several authors refer that the stiffness of the joints does not have a significant contribution for the response at the collapse, which is also valid for static loading (Sarhosis et al. 2015; Giamundo et al. 2014). Moreover, neglecting the contribution provided by the strength of the joints can lead to a conservative response.

2.2 Test setup

The dynamic tests were performed in the National Laboratory of Civil Engineering, Lisbon, Portugal (LNEC), namely in the three axial shake table (Fig. 5d). The setup was carefully designed, aiming at obtaining the relevant outputs associated to the shear failure of the test specimen, with similar conditions to real prototypes and necessary for the performance assessment.

In order to simulate the particular boundary conditions that cause an in-plane shear response of the vault, the special testing device adopted by Rossi et al. (2016) was used. It consists of a frame composed of four steel squared plates, linked to each other by the use of aluminium bar couples hinged at both ends with uniball joints. In this way, the distance between the abutments does not vary and their rotation along the vertical axis was prevented. Moreover, the abutments of the vault were rigidly fixed on the top of four steel squared plates through a hexagonal bar by interlocking (Fig. 5b).

As shown in Fig. 5b, c, the abutments *p1* and *p2* have been fixed using four bolts each, to connect the corresponding steel plates to the flat aluminium surfaces through the threaded holes (Fig. 5b), while *p3* and *p4* were left free to move on the flat aluminium surface above

four spheres each (Fig. 5c). As discussed in Rossi et al. (2016), boundary conditions are a relevant drawback of the test specimen, representing a specific configuration (fully fixed $p1$–$p2$ and completely free $p3$–$p4$), without a lateral wall along the fixed edge, as it is common to find in the real structures. However, the authors consider this configuration to be a representation of the safe side of the reality, with the test specimen that tends to be more deformable.

In Rossi et al. (2016), the displacements were assigned along the Y (longitudinal) direction, through an external actuator, for the quasi-static tests. The instrumentation and boundary conditions used during the shake table tests were similar to those used for the quasi-static tests. At the same time, due to the small geometrical dimensions of the test specimen, specific instrumentation was also implemented. One linear variable displacement transducer ($LDVT_1$) was located at the N–W corner, measuring the relative longitudinal displacement of the movable piers. Six piezoelectric accelerometers (Acc_{1x}, Acc_{1y}, Acc_{1z}, Acc_{2x}, Acc_{2y}, Acc_{2z} in Fig. 5c) were placed at the bottom of the vault to measure the response of the fixed plated, while five variable capacitance unidirectional accelerometers (Acc_{3y}, Acc_{4x}, Acc_{5z}, Acc_{6x}, Acc_{7y}) were placed on the vault, since they are compatible with the dimension of the blocks in terms of dimensions and weight.

Moreover, two optical cameras were used to record the response of the key of the western arch and the movable piers using automatic tracking, respectively, along the plane xy (OP_{1xy}) and yz (OP_{2yz}).

Two video cameras were used to record the tests: one exactly at the top of the test specimen, using scaffolding, and another located in front of the East elevation on a tripod outside of the shake table. From those cameras, the collapse mechanism was evaluated (Sect. 4).

3 Experimental campaign results

In this Section, the main results obtained from both experimental campaigns with the reduced scale vault are presented. First, the monotonic quasi-static tests performed by Rossi et al. (2016) are briefly described. Next, the new dynamic identification tests and shake table tests performed at LNEC are presented.

3.1 Monotonic quasi-static tests

Rossi et al. (2016), simulated the simple shear mechanism of the masonry vault, as shown in Fig. 6, in order to apply in-plane shear distortion. As previously described, on one side, two plates ($p1$ and $p2$) were fixed to the aluminium surface, while plates $p3$ and $p4$ were left free to move. The displacement was applied by an external actuator at the $p4$ plate.

The displacement ds_1 was monitored by means of a LVDT, while the related force Fs_1 was measured by a load cell close to the displacement actuator. The development of the mechanisms up to the collapse was recorded by two high resolution/high frame rate cameras. It was observed that in general all webs show a typical four-hinge asymmetric arch mechanism, opposite in sign. The diagonal shear crack in the extrados can be noted

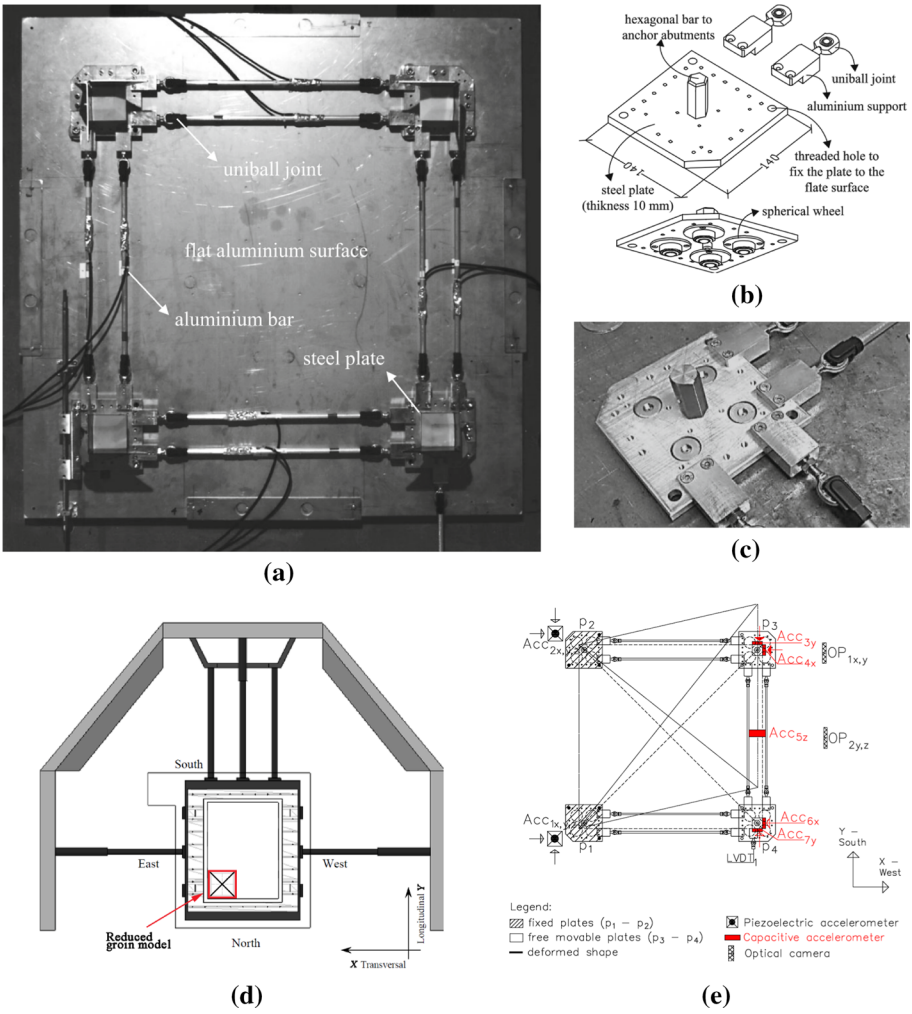


Fig. 5 Experimental setup: **a** movable frame to apply displacements for the quasi-static tests carried out by Rossi et al. (2016); **b**, **c** details of the boundary conditions Rossi et al. (2016) **d** plan with the location of the test specimen (highlighted in red) in the shaking table; **e** instrumentation adopted in the shake table tests (top view)

and the first collapsing web is the one connecting $p3$ and $p4$ where the displacement is applied. The maximum force varies approximately from 13 to 17% of the total weight of the specimen (349.2 N) while the shear distortion (measured by the ratio of the displacement to the free span of the vault) is in the range 3.8–4.8% (Fig. 6).

3.2 Shake table tests

3.2.1 Dynamic identification tests

Dynamic identification tests allow to estimate the modal properties in the elastic regime of the test specimen. In this study, forced vibration tests were performed, in which the input and the response are measured. This kind of test is, characterized by a known input (Ramos 2007; Mendes et al. 2014), namely a "white noise" random signal, with wide frequency range (0.1–40 HZ) and low amplitude (3–8 mm). The test aim at determining the modal parameters of the undamaged and damaged configurations. The amplitudes of the white noise input (here defined in terms of nominal displacement) were increased for evaluating the influence of the amplitude of the signal on the dynamic properties. This is particularly relevant given the use of dry joints, as their stiffness is highly dependent on the normal stress and the structural vault stiffness is also dependent on the crack opening of the joints. The frequencies range from 3.22 Hz (for 8 mm of amplitude) to 4.50 Hz (for 3 mm of amplitude), with a variation of about 0.25 Hz per 1 mm of amplitude. As expected, the increase of the signal amplitude (nominal displacement) causes a decrease in the frequency of the test specimen. The reduction of the frequencies is associated with the opening of the joints, *i.e.* to the damage on the test specimen, which is higher when the amplitude of the input is increased, corresponding to nonlinear behaviour.

In order to verify the sensitivity of the model to the construction process, the test specimen was rebuilt four times, using the same builders, and trying to follow the same procedure. The dynamic identification tests carried out on different days and after different rebuilds of the test specimen present similar frequencies for the same signal amplitude (5 mm), leading to the conclusion that the test specimen exhibits a small scatter of the modal frequencies (between 3.9 and 4.2 Hz), despite the different constructions or environmental conditions. This aspect further validates the methodology adopted for these tests. In addition, the value of 4.0 Hz (for 5 mm of amplitude) was considered as reference frequency of the test specimen because it was a good compromise between the quality of the signal, in terms of peaks to identify the frequency and the very low nonlinear behaviour (opening of the joints).

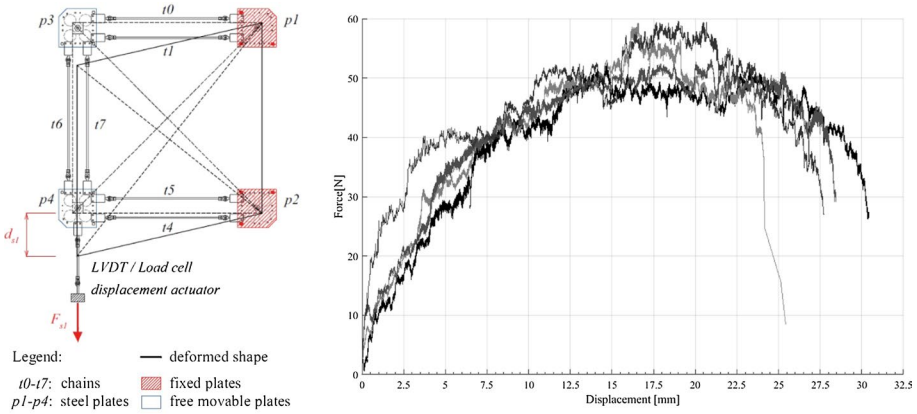


Fig. 6 Test setup and results of the quasi-static tests (Rossi et al. 2016)

The dynamic identification tests were also used to monitor the dynamic properties of the test specimen, in particular the first natural mode of vibration, during the seismic tests. They have been repeated after each seismic test, aiming at identifying small variations in the frequency of the test specimen as an indicator of permanent damage due to movement of the blocks, sometimes not easily identified by the human eye (Sharma et al. 2020).

3.2.2 Seismic tests

In the seismic tests performed in the shake table, two types of ground motions were used, namely the Emilia earthquake and an artificial accelerogram.

The first seismic input motion was recorded by the seismic station located in Mirandola (Station code: MNR) (Italy) (Moretti et al. 2013), which registered the Emilia Romagna's earthquake on the 29th of May 2012 at 06:59:53 (UTC), with a Richter magnitude of 5.8. MNR is the closest station to the epicentre that belongs to the RAN network (managed by the Italian Department of Civil Protection). The second seismic input is an artificial accelerogram compatible with the elastic response spectrum defined by the Italian Code (Ministero delle Infrastrutture e Trasporti 2018), considering the same municipality (Mirandola) and rock type of soil.

Figure 7 presents the elastic response spectrum of the Italian Code NTC 2018 (for the horizontal component) and the spectrum of the artificial accelerogram. The spectrum of the Emilia target input is also plotted in the same figure. The vertical dashed line represents the first natural frequency of the test specimen equal to 4.0 Hz (average between all the dynamic identification tests performed with 5 mm of amplitude), corresponding to 0.25 s, in which the spectral acceleration of the Emilia target input (0.6 g) is about 0.17 g above the spectral acceleration of the Italian Code (0.43 g). This is the main aspect that influences the behaviour of the test-specimen under these two different seismic inputs.

In the same way, Fig. 8 shows the time histories of the selected inputs, which correspond to 100% of the respective seismic action. The Emilia target input is characterised by a duration of 8.93 s. Its peak ground acceleration (PGA) is equal to 284.6 mg and the maximum displacement (PGD) is equal to 31.00 mm, while its root mean square acceleration (RMSA) and root mean square displacement (RMSD) are respectively equal to 72.50 mg and 7.09 mm. The artificial accelerogram presents the same duration, a PGA equal to 173.3 mg, a maximum displacement equal to 16.00 mm, its RMSA has a value of 46.75 mg and the RMSD is equal to 7.87 mm. The two inputs were also subjected to a signal processing using a high pass Butterworth filter with 8 poles and a cut-off frequency equal to 1 Hz.

The duration of the inputs, applied in the seismic tests, was scaled in order to follow the Cauchy-Froude's similitude. To select the corresponding scaling factor, the material values of an ideal prototype, identified during the previous work of this research (see Rossi et al. (2016) for all the data) were taken into consideration. A basic comparison was made through a finite element model (full scale) to evaluate the ratio between the frequencies of the specimen and the prototype. The first frequency corresponds to the measured frequency of the tested specimen (4.0 Hz), while the second was obtained by performing eigenvalue analysis on a finite element model that reproduces the full-scale prototype. Due to the three different scales, which derive from the complexity of the model (namely geometry, density, and deformability), none of the laws was completely respected. However, Cauchy-Froude presents a frequency ratio closer to the expected

nominal relation. Thus, Cauchy-Froude's law was adopted for scaling the duration of the two inputs according to the relation $I^{0.5} = 5^{0.5}$, in which I is the geometric scale factor equal to 5. Following again Cauchy-Froude's law, the acceleration scale factor is unity (Carvalho 1998).

In this study, only the y-longitudinal components (north–south direction), which correspond to the HNN channel of the MNR station for Emilia earthquake, were considered in order to excite the movable piers and induce the shear failure in the vault (Fig. 8).

The use of two different type of inputs (Emilia, impulsive, and Artificial, more regular) was determined by the significative importance of investigating the response with one dominant pulse action and one more regular signal with an almost constant intense phase, expected by the Italian Code (Ministero delle Infrastrutture e Trasporti 2018). Indeed, as stated in literature (e.g. Dejong and Ochsendorf (2010)), it is expected that the primary impulse of an expected ground motion is fundamentally important in predicting the collapse. However, artificial earthquakes have specific characteristics, such as the multiple consecutive impulses and the higher duration of the action, that might have an amplifying effect on the rocking motion, also causing the collapse.

The testing sequence of the vault is presented in Table 2, in which the seismic action was applied with increasing amplitude until collapse and the model was rebuilt 3 times (indicated here as Construction 1 to 3). Before the first and after each seismic test, dynamic identification tests (DIT) were performed, with the amplitude of 5 mm, in order to evaluate the decrease of frequencies as a function of the cumulative damage, which was almost equal to zero until 50% of the Emilia ground motion and until 100% of the artificial ground motion (Table 2). When only a few blocks fell during the test, the test specimen was repaired, in order to keep the same starting point to the test specimen (undamaged test specimen). In the case of Construction 3, the test specimen was not repaired, aiming at simulating a sequence of shocks and the consequent accumulation of damage.

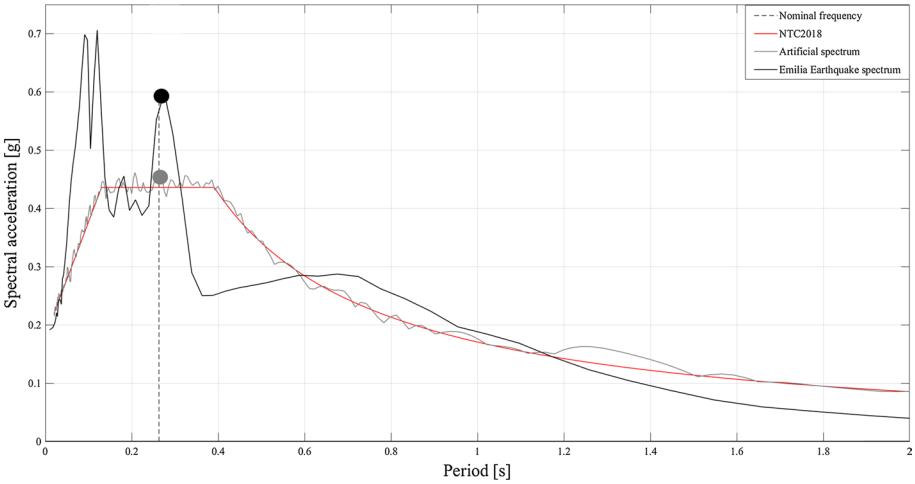


Fig. 7 Elastic response spectra of the selected input signals (Emilia target input and artificial accelerogram) and comparison with the 475-years return period design spectrum for Mirandola according to NTC2018. The periods are scaled according to the similitude relationships

4 Analysis of the results

To compare the results of the static tests carried out by Rossi et al. (2016) with the shake table tests (ST), the analysis of collapse mechanism was adopted, in which a sequence of photos, with the number and locations of the hinges, was used. Looking at Fig. 9, the centre of the vault is the first to collapse in both tests, due to its geometrical configuration and the verticality of the joints. The shear failure is the first to occur and it is represented by crack opening along the diagonals. It is noted that, in the quasi-static tests, the diagonal cracks appear only along the S–E direction, between the movable piers, due to the monotonic sign of the action. On the other hand, for the shaking table tests, those cracks appear both at N–W and S–W diagonals, between the fixed piers, due to the cyclic movement caused by the action (accelerogram). Similarly, during the shake table tests, the hinges started to appear from the East side of the test specimen between $p1$ and $p2$, the fixed piers, while during the quasi-static tests the first hinge occurred between the movable piers (west side) $p3$ and $p4$, resulting in a mirrored mechanism. This aspect occurs because the movable edge can recover part of the damage, namely closing the joints during the shaking table tests (cyclic movement). In contrast, in the fixed edge, which is more rigid, the opening of the joints is larger. For the quasi-static tests, the joints of the movable edge open without the possibility of recovering the damage (monotonic movement), resulting as the first edge to collapse. Moreover, it is worth noting that the actuator used in the quasi-static tests constituted a constrain, making the boundary conditions slightly different from the dynamic tests.

Analysing the dynamic test results, the external edges (North and West side) continue to stand, even when the other sides already fell down. The hinges are located at the East elevation, both for the Emilia and the artificial inputs (Fig. 9).

The steel plates at the corners make the boundaries of the shell of the vault stiffer and, therefore, two hinges occur where the steel plates do not act anymore. This is in agreement with the prediction of Oppenheim (1992) and De Lorenzis et al. (2007), based on the minimum energy formulations. Considering the response obtained from

Table 2 List of shaking table tests carried out on the reduced scale vault (chronological order)

	Tests with Emilia input		Tests with Artificial input	
	DIT	Seismic action	DIT	Input
	Frequency [Hz]	% of action and notes	Frequency [Hz]	% of action and notes
Construction 1	4.10	10%	4.00	50%
	4.10	25%	4.00	75%
	4.00	50%—recovered	4.00	100%
	3.91	75%- collapse	3.90	125%
			3.71	150%
			3.35	200%—collapse
Construction 2	3.61	60%—collapse (*initial minor damage)		
Construction 3	4.00	55%—unrecovered		
	3.42	25%—aftershock1		
	3.22	35%—aftershock2		

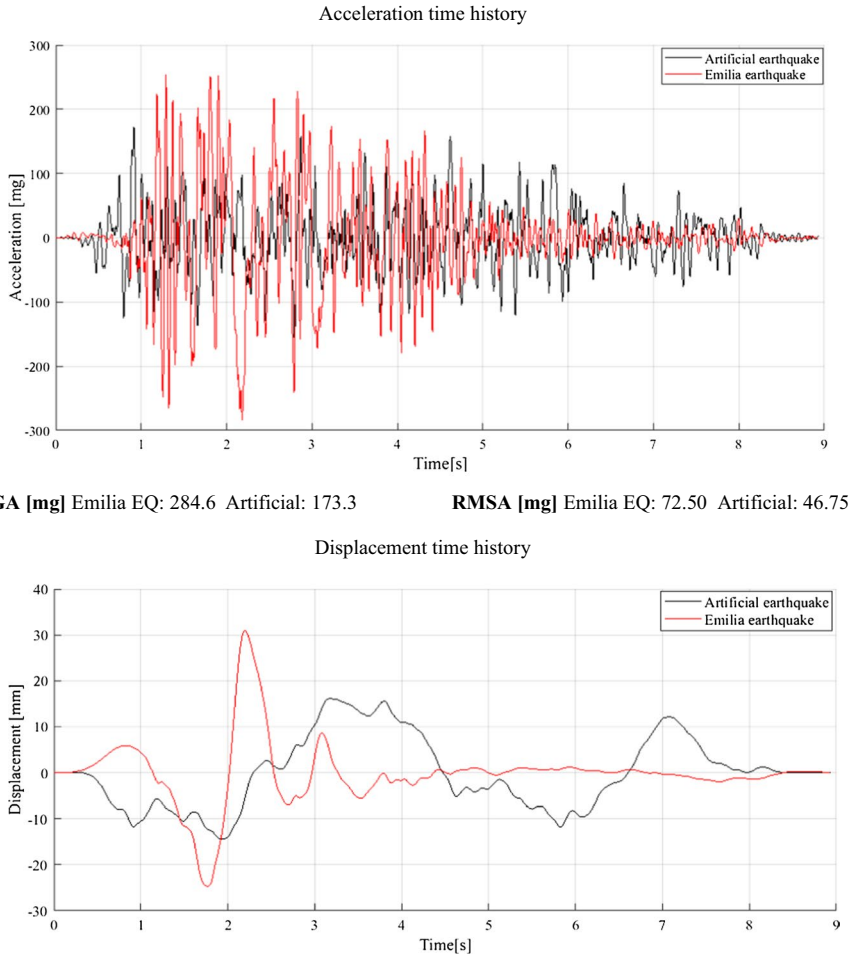


Fig. 8 Scaled time histories of accelerations and displacements for the reduced test specimen. (Emilia and artificial inputs—amplitude equal to 100%)

the shake table tests, the arch mechanism is clear (four hinges), and it firstly appears between the fixed supports (Fig. 9).

As widely observed for the behaviour of similar structures like arches, different loading distribution leads to a different response. In the case of the vault, the three-dimensional complexity of the structure amplifies this concept. Indeed, the core aspect of this research is that the quasi-static tests are mainly associated with the gravitational set of loads, while the shake table tests consider the inertial force acting on the structure.

The main objective is to assess the groin-vault behaviour independently from the load type and then to stress the fact that for this kind of structures, the nonlinear static approach represents an approximation of the reality that does not replicate all loading scenarios. At the same time, even two different inputs in the shaking table lead to different quantitative conclusions due to the spectra contents of the seismic action itself.

Table 3 Incremental dynamic testing sequence with the respective peak ground acceleration (PGA), peak ground velocity (PGV) and peak ground displacement (PGD)

Emilia input					Artificial input				
Test input %	PGA [mg]	PGV [mm/s]	PGD [mm]	Damage notes	Test input %	PGA [mg]	PGV [mm/s]	PGD [mm]	Damage notes
10	3.55	7.23	0.31	–	10	1.23	0.53	0.16	–
25	19.17	17.22	1.96	–	25	8.72	3.75	0.99	–
35	33.70	32.67	3.87	–	50	39.30	14.52	3.99	–
50	70.65	64.58	7.94	Fall of the key blocks	75	94.27	32.47	8.99	–
55	84.85	77.80	9.53	Opening of the diagonal crack (NW–SE)	100	172.30	58.15	16.10	–
60				Collapse (problems in the setup)	125	344.19	95.80	25.07	Fall of the key blocks
75	160.10	139.47	17.67	Collapse	150	435.12	135.72	36.27	Opening of the diagonal crack (W–S)
					200	763.7	241.21	64.70	Collapse

Regarding the comparison between the two ground motions used during the shake table tests, and as shown in Table 3, the specimen remained undamaged until the scaling factor of 75% and 200% for the Emilia and artificial inputs, respectively.

As previously referred, it is possible to notice that the impulsive nature of the Emilia earthquake, caused a rapid collapse of the vault, in comparison with the artificial accelerogram (Table 3). However, the type of collapse mechanism remains the same, in terms of the evolution of damage and formation of the hinges (Fig. 10). Both types of seismic action show a clear shear behaviour, which occurs along the diagonals that join p_2–p_4 and p_1–p_3, due to the positive and negative direction of the accelerations at the base. It is notable also that the hinges interfere only with the parallel edges (East before and West later), while the transversal webs are not involved in the collapse, and they keep a simple-arch behaviour until the end of the tests. These observations are valid for every amplitude of the shake table tests, starting from the value of amplitudes that could cause a more relevant state of damage. For the sake of clarity and conciseness, only the collapse mechanism and the time series of the displacements before reaching the collapse itself are compared, namely for the 75% of the Emilia input and the 200% of the artificial input (Figs. 10 and 11).

From the time series of the displacements of the movable piers (Fig. 11), referred at the amplitude of the collapse, the major peaks occurred between 2.5 and 3.5 s of the duration.

The performance of the test specimen in terms of displacements and accelerations require a more detailed analysis. It is confirmed that the impulsive nature of the Emilia earthquake significantly influences the response of the structure and, even with lower values of spectral acceleration, induces earlier damage in the structure. Acceleration and displacement response spectra of the different time histories, all built for a damping of 5%, are very different in content and peaks (Fig. 12).

Table 4 shows some relevant outputs associated with the recorded response of the structure. Besides the fact that the content of the two inputs is different, the

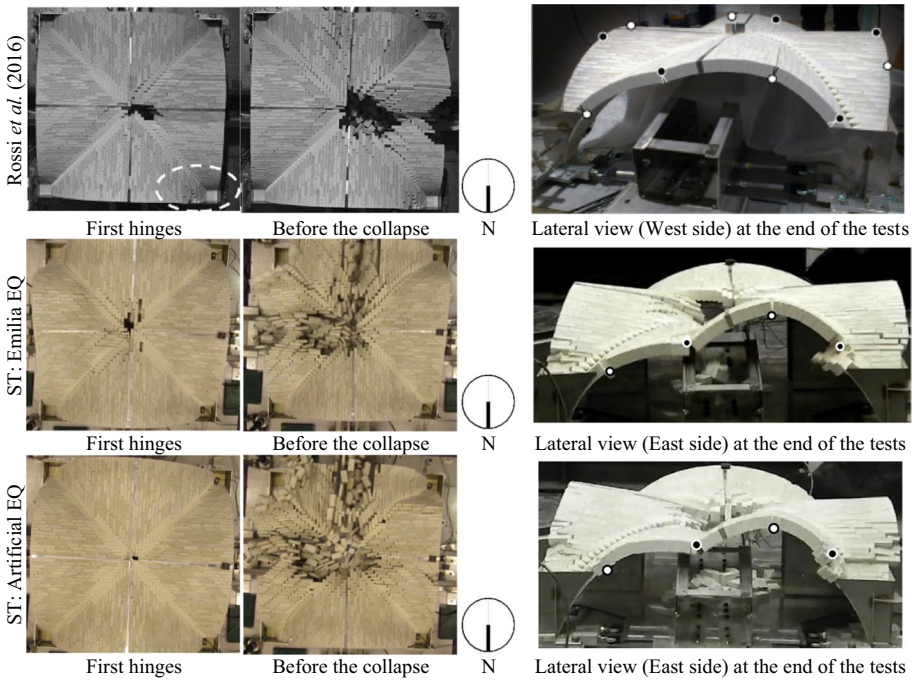


Fig. 9 In-plane shear mechanism: pictures of the test (white circles indicate the location of the hinges at the extrados, while black circles indicate the location of the hinges at the intrados)

displacements recorded by the movable piers showed good consistency for all shake table tests. The values of drifts (ratio between the relative displacement and the span), recorded by the optical camera and the LVDT, placed respectively above the movable piers $p3$ and $p4$, ranges from 5.12 to 7.17%, for both inputs. The average value is about 6%, either for the Emilia input or the artificial input at the collapse, independently of the value of PGA. It is noted that the difference between the two values obtained for the different types of inputs is less than 1% for the optical camera and about 0.1% for the LDVT. From the drifts, it is possible to conclude that under seismic motion the limit drift value that can cause the collapse is equal to 6%. The ultimate drift value measured in the quasi-static tests was about 4.3% of its lateral edge and it corresponds to a conservative result, in comparison with the results obtained from the shaking table tests.

It has been shown in the past, *e.g.* for masonry building, and here confirmed, that dynamic drifts are larger than quasi-static (Abrams et al. 2017; Lagomarsino 2015; Vasconcelos 2005; Gaetani et al. 2017).

For an additional comparison between the types of input, the hysteretic behaviour of the reduced-scale vault is presented in Fig. 13, in terms of a relation between the shear forces/horizontal inertial forces and the displacements. The shear forces developed in the structures, as well as the displacement, have been analysed based on the recorded acceleration and displacement time-histories. The base shear coefficient was calculated by dividing the inertial force associated with each web of the vault by its self-weight. Inertial forces associated with the webs of the vault were calculated by assuming the mass of the reference web to be lumped at the recording accelerometers. In fact, due

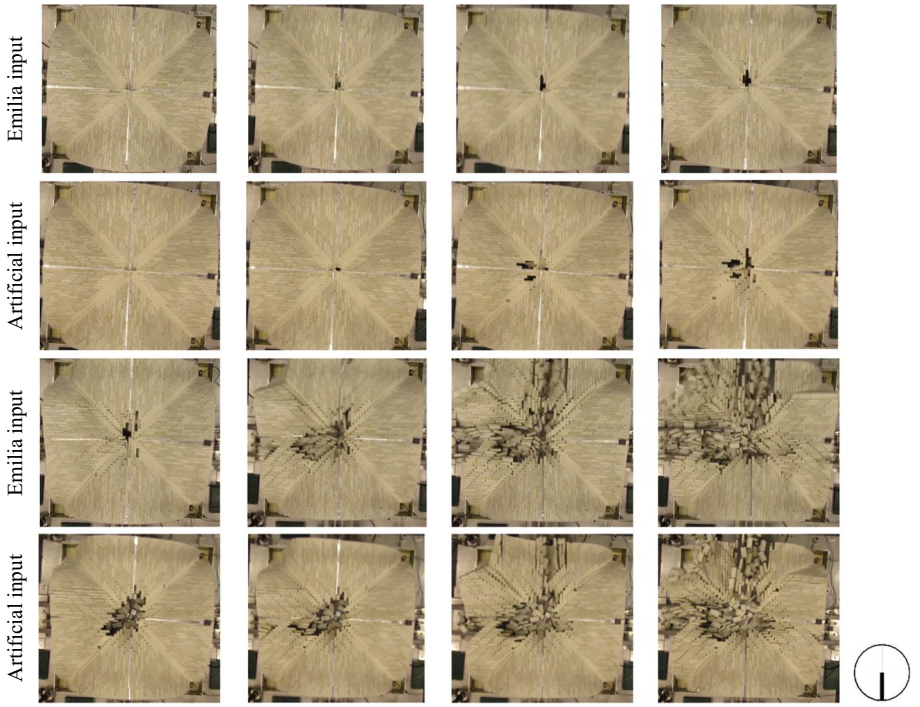


Fig. 10 Damage progression of the test specimen during the intense phase of the Emilia seismic input 75% vs. the artificial input (200%) (5 frames/s). (Left side: fixed supports $p1$–$p2$; right side: movable supports $p3$–$p4$)

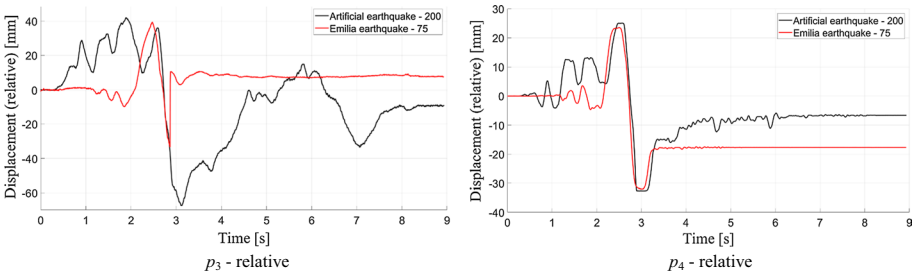


Fig. 11 Time series of the relative displacements of the movable piers ($p3$ and $p4$) at the collapse for Emilia 75% and Artificial 200%

to the geometrical symmetry of the test specimen, the mass associated with each web corresponds to ¼ of the total mass of the test specimen. The inertia forces were computed for each shake table test but, for sake of simplicity, only the most representative scenarios are presented in Fig. 13. The shear coefficient was plotted versus the longitudinal displacement placed at the top of the west arch, measured by the optical camera OP_2. Figure 13a, which refers to stages with the lower amplitudes, represents a linear elastic phase with a very low value of excitation. This behaviour is associated with the

Table 4 Tests results for each dynamic input and the quasi-static tests

Type of input (at the level of the collapse)	Test input %	PGA [m/s^2]	PGV [mm/s]	PGD [mm]	Maximum ABS displacement *p3* (Optical camera) [mm]	Drift [%]	Maximum REL displacement *p4* (LVDT) [mm]	Drift [%]	Drift average [%]
Emilia input	75	1.6	139.5	17.8	44.8	7.2	32.0	5.1	6.2
Artificial input	200	7.5	241.2	64.7	39.1	6.3	32.6	5.2	5.7
Quasi-static tests	Collapse						24.7–31.2	3.8–4.8	

undamaged configuration of the vault, namely when the openings of the joint do not lead to the fall of blocks. The linear range is evident even for the hysteretic curves plotted at the amplitude of the collapse (Fig. 13b), in which two vertical lines are associated with the initial phase. Then, very high nonlinear behaviour, for both inputs, is observed. As noticed before in the evaluation of the drifts, the hysteretic curves also show similarities when considering the Emilia input and the artificial input. The scattered behaviour of the curve is marked by the different slopes of the curves, which represents a change in terms of stiffness and permanent deformation. Emilia input and artificial input show a quite similar nonlinear behaviour but mirrored in sign. In general, when the artificial input is applied, the structure is characterized by a higher capacity in terms of shear coefficient, while with the Emilia input the structure shows a higher deformation. Despite the different response in terms of displacements, when compared with the quasi-static tests, it was observed that the maximum strength capacity ranged between 13 and 17% of the force/weight ratio, which is compatible with the value obtained by the shake table tests (Fig. 13b).

Figure 14 shows the plots for the incremental dynamic tests performed in the shake table tests, for the Emilia input and the artificial input. The maximum base shear at each stage of testing and the corresponding value of displacement recorded by the sensor located at the key of the west arch (OP_{2y}), occurring at the same instant of time, is reported. The first points show the linear range of response, despite the difficulty to observe the differences in terms of stiffness due to the low level of amplitude. During this kind of tests, it is normal to get a better response for a medium value of amplitude and intensity. The tests with the Emilia input and the artificial input show a similar capacity in terms of base shear and deformations. This outcome is in line with what was obtained in previous research on reduced-scale test specimens (Tomaževič 1999).

The differences in terms of inputs and response can be also identified in Fig. 15. As Candeias et al. (2016) stressed, a straight line with a 1:1 slope means that the absolute accelerations are equal in the base and the other selected points of the test specimen. This means a rigid body motion, whereas if the slope is higher means that there is dynamic amplification in the test specimen. Finally, if there is an exponential increase of the plots with the increase of the input motion intensity, it means that the test specimen has reached the nonlinear behaviour. Looking at Fig. 15a, c, it is possible to observe the dynamic behaviour of the vault for the Emilia input. It can be defined as linear from the tests with 10% to 60%, except for the point for the 55%, which corresponds to the third construction (Table 2). This could be associated with some relative movements during the recording state of the sensor or due to the construction process. Before the collapse, firstly achieved with 75% of the seismic motion, it is possible to notice an exponential increase significantly evident from the accelerations recorded on the top of the movable piers (Acc_{3y}, Acc_{7y}), less remarkable for the ones placed on the fixed piers (Acc_{1y}, Acc_{2y}).

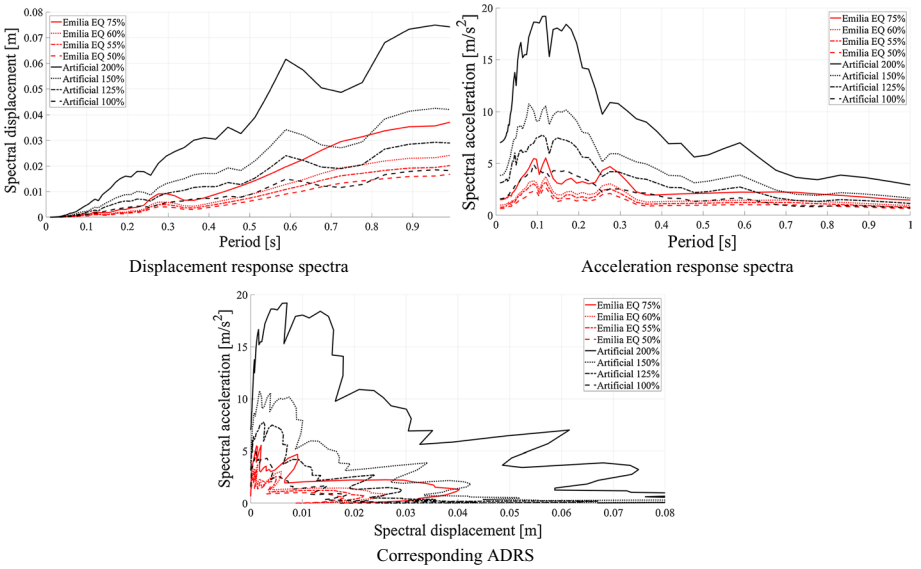


Fig. 12 Displacement and acceleration response spectra for the signals measured at the shake table for the two inputs: Emilia input (left) and artificial input (right)

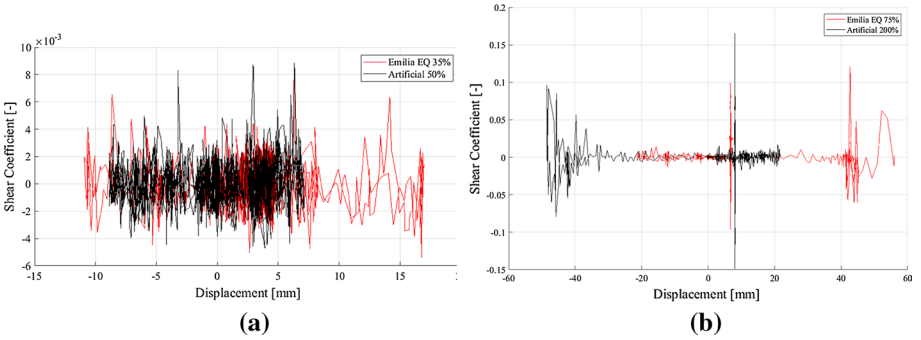


Fig. 13 Hysteretic behaviour (base shear coefficient vs top arch displacement) for different stages of testing: Emilia EQ 35% vs artificial EQ 50% (**a**) and Emilia EQ 75% vs artificial EQ 200% (at the collapse) (**b**)

On the other hand, for what concerns the artificial input, Fig. 15b, d), the linear range was identified between the 10% and the 120% of the ground motion, while the exponential rate is mainly localised on the last two sequences of tests (150% and 200%), when effectively the severe damage occurred.

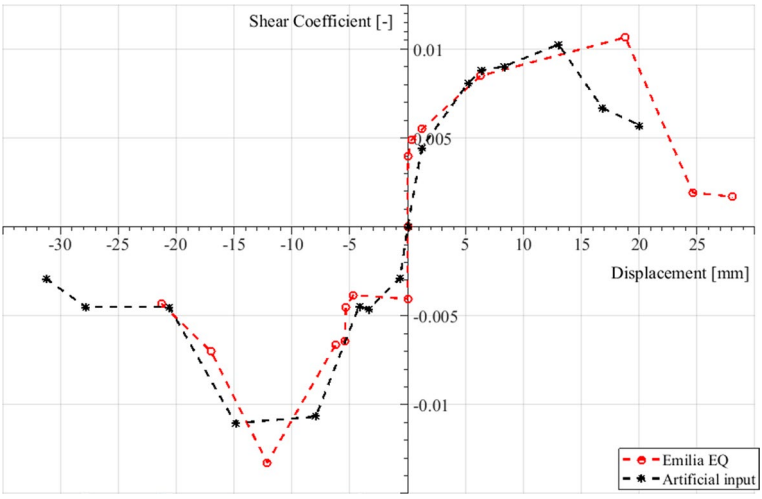


Fig. 14 Experimental capacity curve, in terms of base shear coefficient and displacement at the key of the arch (OP_{2y})

5 Conclusions

This work describes a comprehensive experimental investigation composed by shake table tests developed for the characterisation of the shear failure of a reduced scale test specimen (1:5) of a 3D printed groin vault. Two experimental campaigns using different approaches of loading were discussed, namely: (a) monotonic quasi-static tests, previously performed by Rossi et al. (2016); (b) shake table tests applying the Emilia earthquake (2012) and an artificial accelerogram for the same zone. The shake table tests include also dynamic identification tests.

The objectives of this work were to evaluate the variation of the response considering the two different types of loading (quasi-static and dynamic) and the two different types of seismic action applied in the shake table tests (recorded vs artificial accelerograms). The results were mainly compared in terms of maximum load capacity, drift/displacement capacity and collapse mechanisms. Damage and collapse mechanism. One potential objective was represented by the characteristics of the test specimen, rebuildable which can be used for several experimental applications.

The results obtained from the dynamic identification tests, performed before and after each seismic shake table test, allowed to evaluate the reduction of frequencies of the test specimen, which can be used as an indicator of the damage. The development of a four-hinge symmetric mechanism was observed in two webs during the quasi-static tests. On the other hand, a similar mirrored mechanism was obtained for the shake table tests, but the first location of the hinges appears between the fixed piers of the vault, associated with the stiffer behaviour of the fixed edge.

The displacement/drift levels achieved in the shake table tests were higher (about 6% of the span) than the ultimate displacement/drift obtained from quasi-static tests (about 4% of the span), using the same reduced scale vault of Rossi et al. (2016). This aspect allows to

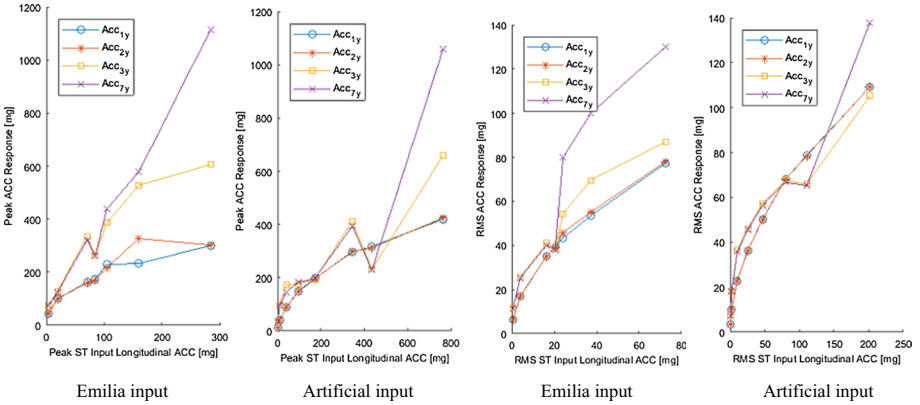


Fig. 15 Peak and RMS acceleration of the response for the reduced-scale vault in the longitudinal direction

conclude that, in general, the monotonic approach is more conservative than the dynamic approach. This is according to the expected, but the novelty of the paper is that this statement was studied only in case of walls or simpler structures, but it was never experimentally investigated before for groin vault structures.

The capacity in terms of base shear was similar in both tests. The differences in terms of collapse between the Emilia earthquake and the artificial seismic input are influenced by the spectral acceleration of the Emilia input that is about 0.17 g above the spectral acceleration of the Italian Code (0.43 g), or the first period of the test specimen. This stresses the fact that, according to the most recent codes, a significant number of records must be selected in order to allow a better description of the safety of the structure (Lagomarsino and Cattari 2015).

Finally, this study, complemented by the dynamic identification tests, provides useful data for the development and calibration of reference numerical models, adopting different strategies, which then allow to evaluate the seismic behaviour of vaults with different geometry and seismic action. Moreover, this research provides a step for further investigations, which may contain more realistic boundary and loading conditions, such as the presence of the lateral wall, the presence of filling material, and the three components of the seismic actions.

Acknowledgements The authors are grateful to the National Laboratory of Civil Engineering and all the technicians for providing the experimental data for the shake table tests. This work was partly financed by FCT – Foundation for Science and Technology within the scope of the SERA.TA project "Seismic Response of Masonry Cross Vaults: Shaking table tests and numerical validations" and the PhD grant SFRH/BD/136831/2018. Finally, the authors would like to thank the Reviewers who contributed to significantly improve the overall quality of this paper.

Declaration

Conflict of interest The authors certify that they have no affiliations with or involvement in any organization or entity with any financial interest, or non-financial interest in the subject matter or materials discussed in this manuscript.

References

Abraham D (1934) Viollet-Le-Duc et Le Rationalisme Médiéval. Bull Monumental. https://doi.org/10.3406/bulmo.1934.10100

Abrams D, AlShawa O, Lourenço PB, Sorrentino L (2017) Out-of-plane seismic response of unreinforced masonry walls: conceptual discussion, research needs, and modeling issues. Int J Archit Herit 11(1):22–30. https://doi.org/10.1080/15583058.2016.1238977

Arcidiacono V, Cimellaro GP, Piermarini E, Ochsendorf JA (2016) The dynamic behavior of the Basilica of San Francesco in Assisi using simplified analytical models. Int J Archit Herit 10(7):938–953. https://doi.org/10.1080/15583058.2016.1158333

Baraccani S, Zauli L, Theodossopoulos D, Silvestri S (2020) Experimental test on a fibre-reinforced scaled cross vault subjected to in-plane shear displacements at the springings. Constr Build Mater 265:120305. https://doi.org/10.1016/j.conbuildmat.2020.120305

Bertolesi E, Jose MA, Paula R, Pedro AC (2019) Research and practice on masonry cross vaults—a review. Eng Struct 180(October 2018):67–88. https://doi.org/10.1016/j.engstruct.2018.10.085

Bianchini N, Nuno M, Paulo BL, Chiara C, Michela R (2019) Seismic assessment of masonry cross vaults through numerical nonlinear static and dynamic analysis. In: COMPDYN 2019 7th ECCOMAS thematic conference on computational methods in structural dynamics and earthquake engineering, edited by M. Papadrakakis and M. Fragiadakis, 600–612. Crete, Greece. https://doi.org/10.7712/120119.6942.18709

Borri A, Marco C, Andrea V (2002) New materials for strengthening and seismic upgrading interventions. International Workshop Ariadne 10, no. 1954: 1–24. http://itecwrap.com/PDF_BASE_1/Seismicw10_borri

Briccoli B, Silvia IF, Giovanna R, Luisa R, Marta R (2002) Costruzioni voltate in muratura prototipo volta a crociera

Calderini C, Lagomarsino S (2015) Seismic response of masonry arches reinforced by tie-rods: static tests on a scale model. J Struct Eng 141(5):4014131–4014137. https://doi.org/10.1061/(ASCE)ST.1943-541X.0001079

Calderini C, Lagomarsino S, Rossi M, De Canio G, Mongelli M, Roselli I (2015) Shaking table tests of an arch-pillars system and design of strengthening by the use of tie-rods. Bull Earthq Eng 13(1):279–297. https://doi.org/10.1007/s10518-014-9678-x

Candeias PX, Costa AC, Mendes N, Costa AC, Lourenço PB (2016) Experimental assessment of the out-of-plane performance of masonry buildings through shaking table tests experimental assessment of the out-of-plane performance of masonry buildings. Int J Archit Herit 11(1):31–58. https://doi.org/10.1080/15583058.2016.1238975

Cangi G (2009) Ruolo Delle Volte e Tecniche Di Consolidamento. 2

Cangi G (2012) Manuale Del recupero strutturale e antisismico, 2nd edn. DEI, Rome

Carfagnini C, Baraccani S, Silvestri S, Theodossopoulos D (2018) The effects of in-plane shear displacements at the springings of gothic cross vaults. Constr Build Mater 186:219–232. https://doi.org/10.1016/j.conbuildmat.2018.07.055

Carvalho E (1998) Seismic testing structures. In: 11th European Conference on Earthquake Engineering

Cattari S, Sonia R, Sergio L (2008) Modelling of vaults as equivalent diaphragms in 3D seismic analysis of masonry buildings. In: Structural analysis of historical constructions, edited by Dina Francesca D'Ayala and Fodde, 517–24. London: Taylor & Francis Group.

Ceradini V (1996) Modelli sperimentali Di Volte in Tufo e Mattoni. In: La Meccanica Delle Murature Tra Teoria e Progetto, 157–66. Messina

Como M (2013) Statics of historic masonry constructions. Vol. 1. Springer series in solid and structural mechanics. Springer, Berlin. https://doi.org/10.1007/978-3-642-30132-2

Croci G (2000) General methodology for the structural restoration of historic buildings: the cases of the tower of pisa and the Basilica of Assisi. J Cult Herit 1(1):7–18. https://doi.org/10.1016/S1296-2074(99)00119-3

D'Ayala DF (2005) Force and displacement based vulnerability assessment for traditional buildings. Bull Earthq Eng 3(3):235–265. https://doi.org/10.1007/s10518-005-1239-x

D'Ayala DF, Tomasoni E (2011) Three-dimensional analysis of masonry vaults using limit state analysis with finite friction. Int J Archit Herit 5(2):140–171. https://doi.org/10.1080/15583050903367595

Dejong MJ, Ochsendorf JA (2010) Dynamics of in-plane arch rocking: an energy approach. Proc Inst Civ Eng Eng Comput Mech 163(3):179–186. https://doi.org/10.1680/eacm.2010.163.3.179

Doglioni F, Moretti A, Petrini V (1994) Le Chiese e Il Terremoto. Dalla Vulnerabilità Constatata Nel Terremoto Del Friuli Al Miglioramento Antisismico Nel Restauro. Verso Una Politica Di Prevenzione. Trieste: Lint Editoriale Associati

Faccio P, Foraboschi P, Siviero E (1999) Volte in muratura con Rinforzi in FRP (in Italian). L'edilizia 7(8):44–50

Fagone M, Rotunno T, Bati SB, Bati SB (2016) The groin vaults of St. John Hospital in Jerusalem: an experimental analysis on a scale model. Int J Archit Herit 10(May):903–918. https://doi.org/10.1080/15583058.2016.1158331

Formenti C (1893) La Pratica Del Fabbricare per l'ingegnere. Ulrico Hoepli, Milano

Foti D (2015) Structural behaviour of historical stone arches and vaults : experimental tests and numerical analyses. Key Eng Mater 2:43–48.

Foti D, Vacca V, Facchini I (2018) DEM modeling and experimental analysis of the static behavior of a dry-joints masonry cross vaults. Constr Build Mater 170:111–120. https://doi.org/10.1016/j.conbuildmat.2018.02.202

Gaetani A, Paulo BL, Monica M, Giorgio M, Monica M (2017) Shaking table tests and numerical analyses on a scaled dry-joint arch undergoing windowed sine pulses. Bull Earthq Eng. https://doi.org/10.1007/s10518-017-0156-0

Gaetani A, Giorgio M, Paulo BL, Giancarlo M (2015) Masonry cross vaults: an overview of the historical developments. AID Monuments 2015. Materials Techniques Restoration for Architectural Heritage Reusing, 589–601.

Gaetani A, Monti G, Lourenço PB, Marcari G (2016) Design and analysis of cross vaults along history. Int J Archit Herit 10(7):841–856. https://doi.org/10.1080/15583058.2015.1132020

Giamundo V, Sarhosis V, Lignola GP, Sheng Y, Manfredi G (2014) Evaluation of different computational modelling strategies for the analysis of low strength masonry structures. Eng Struct 73:160–169. https://doi.org/10.1016/j.engstruct.2014.05.007

Giovanetti (2000) Manuale Del Recupero Del Comune Di Città Di Castello. Rome (in Italian): DEI.

Heyman J (1969) The safety of masonry arches. Int J Mech Sci 11(November 1968):363–385. https://doi.org/10.4324/9781315249513-20

Heyman J (1982) The masonry arch. Edited by Horwood. Ellis Horwood Limited, Chichester

Heyman J (1995) The stone skeleton: structural engineering of masonry architecture. Edited by Cambridge University Press. Cambridge University Press, Cambridge

Huerta S (2004) Arcos, Bóvedas y Cúpulas: Geometría y Equilibrio En El Cálculo Tradicional de Estructuras de Fábrica. Instituto Juan de Herrera, Madrid, España

Lagomarsino S (2015) Seismic assessment of rocking masonry structures. Bull Earthq Eng 13(1):97–128. https://doi.org/10.1007/s10518-014-9609-x

Lagomarsino S, Cattari S (2015) PERPETUATE guidelines for seismic performance-based assessment of cultural heritage masonry structures. Bull Earthq Eng 13(1):13–47. https://doi.org/10.1007/s10518-014-9674-1

Lagomarsino S, Resemini S (2009) The assessment of damage limitation state in the seismic analysis of monumental buildings. Earthq Spectra 25(2):323–346. https://doi.org/10.1193/1.3110242

De Lorenzis L, Dejong MJ, Ochsendorf JA (2007) Failure of masonry arches under impulse base motion. Earthq Eng Struct Dynam 36(14):2119–2136. https://doi.org/10.1002/eqe.719

Lourenço PB, Ramos LF (2004) Characterization of cyclic behavior of dry masonry joints. J Struct Eng 130(5):779–786. https://doi.org/10.1061/(ASCE)0733-9445(2004)130:5(779)

Mark R, Abel JF, O'Neill K (1973) Photoelastic and finite-element analysis of a quadripartite vault. Exp Mech 13(8):322–329. https://doi.org/10.1007/BF02322391

De Matteis G, Mazzolani FM (2012) The Fossanova church: seismic vulnerability assessment by numeric and physical testing. Int J Archit Herit Conserv Anal Restor. https://doi.org/10.1080/15583050903078903

De Matteis G, Daniela C, Jafar R (2019) Masonry vaults: architectural evolution, structural behaviour and collapse mechanisms. In: 7th structural engineers world congress. Istanbul

Mcinerney J, Dejong MJ (2015) Discrete element modeling of groin vault displacement capacity. Int J Archit Herit 9(8):1037–1049. https://doi.org/10.1080/15583058.2014.923953

Mendes N, Paulo BL, Alfredo CC (2014) Shaking table testing of an existing masonry building: assessment and improvement of the seismic performance. Earthq Eng Struct Dyn 43(August 2013):247–266. https://doi.org/10.1002/eqe

Milani G, Rossi M, Calderini C, Lagomarsino S (2016) Tilting plane tests on a small-scale masonry cross vault: experimental results and numerical simulations through a heterogeneous approach. Eng Struct 123:300–312. https://doi.org/10.1016/j.engstruct.2016.05.017

Miltiadou-Fezans A (2008) A multidisciplinary approach for the structural restoration of the katholikon of dafni monastery in Attica Greece. In: Structural analysis of historical constructions, edited by Dina Francesca D'Ayala and Fodde, 71–87. Taylor & Francis Group, London

Ministero delle Infrastrutture e Trasporti. 2018. Capitolo 3 - NTC 2018 - Azioni sulle costruzioni, issued 2018.

Modena C (2020) Recent advances of Italian recommendations and standards on structural safety of existing masonry structures. In: Brick and block masonry—from historical to sustainable masonry, 42–57. https://doi.org/10.1201/9781003098508-5

Mousavian E, Casapulla C (2020) The role of different sliding resistances in limit analysis of hemispherical masonry domes. Frattura Ed Integrita Strutturale 14(51):336–355. https://doi.org/10.3221/IGF-ESIS.51.25
National Civil Protection Service (2013) Manuale per La Compilazione Della Scheda per Il Rilievo Del Danno Ai Beni Culturali, Chiese - Modello A-DC. Ed. by Simona Papa and Giacomo Di Pasquale
Oppenheim IJ (1992) The masonry arch as a four-link mechanism under base motion. Earthq Eng Struct Dyn 21(11):1005–1017. https://doi.org/10.1002/eqe.4290211105
Podestà S, Anna Brignola E, Curti SP, Lemme A (2010) Damage assessment and seismic vulnerability of churches: the Abruzzo earthquake. Ingegneria Sismica XXVII 1:21–35
Pulatsu B, Ece E, Eduardo MB, Paulo BL (2019) In-plane static response of dry-joint masonry arch-pier structures. AEI 2019: Integrated building solutions—The National Agenda—proceedings of the architectural engineering national conference 2019, no. April: 240–48. https://doi.org/10.1061/9780784482261.028.
Ramos LF (2007) Damage identification on masonry structures based on vibration signatures. Universidade do Minho, Minho
Regione T (2003) Istruzioni Tecniche per l'interpretazione Ed Il Rilievo per Macroelementi Del Danno e Della Vulnerabilità Sismica Delle Chiese. Venzone: ARX s.c.r.l.
Rossi M, Calderini C, Lagomarsino S (2016) Experimental testing of the seismic in-plane displacement capacity of masonry cross vaults through a scale model. Bull Earthq Eng 14(1):261–281. https://doi.org/10.1007/s10518-015-9815-1
Rossi M, Chiara C, Sergio L, Gabriele M (2015) Seismic response of masonry vaulted structures: experimental and numerical modelling. In: 9th International Masonry Conference, edited by Paulo B Lourenço, Barry A Haseltine, and Graça Vasconcelos. Universidade do Minho, Guimarães
Rossi M, Chiara C, Ivan R, Marialuisa M, De Gerardo C, Sergio L (2020) Seismic analysis of a masonry cross vault through shaking table tests: the case study of the dey mosque in Algiers. Earthq Struct 18(1):57–72. https://doi.org/10.12989/eas.2020.18.1.057
Rossi M, Cristián CB, Van Tom M, Philippe B (2017a) Collapse analysis of unreinforced masonry vaults using 3D-printed scale-model testing. In: 7th international conference on advances in experimental structural engineering collapse
Rossi M, Barentin CC, Van Mele T, Block P (2017b) Experimental study on the behaviour of masonry pavilion vaults on spreading supports. Structures 11(May):110–120. https://doi.org/10.1016/j.istruc.2017.04.008
Sanabria SL (1982) The mechanization of design in the 16th century: the structural formulae of Rodrigo Gil de Hontañón. J Soc Archit Hist 41(4):281–293. https://doi.org/10.2307/989800
Sarhosis V, Garrity SW, Sheng Y (2015) Influence of brick-mortar interface on the mechanical behaviour of low bond strength masonry brickwork lintels. Eng Struct 88(April):1–11. https://doi.org/10.1016/j.engstruct.2014.12.014
Shapiro EE (2012) Collapse mechanisms of small-scale unreinforced masonry vaults. Master thesis, Massachusetts Institute of Technology. http://hdl.handle.net/1721.1/72648.
Sharma S, Tomassetti U, Grottoli L, Graziotti F (2020) Two-way bending experimental response of urm walls subjected to combined horizontal and vertical seismic excitation. Eng Struct 219(July):110537. https://doi.org/10.1016/j.engstruct.2020.110537
Theodossopoulos D, Sinha BP, Asce M, Usmani AS, Asce M, Usmani AS (2003) Case study of the failure of a cross vault: church of holyrood abbey. J Archit Eng 9(3):109–117. https://doi.org/10.1061/(ASCE)1076-0431(2003)9:3(109)
Theodossopoulos D, Sinha BP, Usmani AS, Macdonald AJ (2002) Assessment of the structural response of masonry cross vaults. Strain 38(3):119–127. https://doi.org/10.1046/j.0039-2103.2002.00021.x
Tomaževič M (1999) Earthquake-resistant design of masonry buildings. Edited by Imperial College Press, vol 1. Imperial College Press, London
Torres B, Elisa B, Pedro AC, Juan JM, Jose MA (2019a) A full-scale timbrel cross vault subjected to vertical cyclical displacements in one of its supports. Eng Struct 183(July 2018):791–804. https://doi.org/10.1016/j.engstruct.2019.01.054
Torres B, Bertolesi E, Moragues JJ, Calderón PA, Adam JM (2019b) Experimental investigation of a full-scale timbrel masonry cross vault subjected to vertical settlement. Constr Build Mater 221:421–432. https://doi.org/10.1016/j.conbuildmat.2019.06.015
Vasconcelos G (2005) Experimental investigations on the mechanics of stone masonry: characterization of granites and behavior of ancient masonry shear walls. Universidade do Minho, Minho
Williams MS, Alejandra A, Victoria L, Yip F (2012) Model scale shaking table tests on masonry barrel and cross vaults. In: 15 WCEE, Lisbon

Publisher's Note Springer Nature remains neutral with regard to jurisdictional claims in published maps and institutional affiliations.

Authors and Affiliations

N. Bianchini[1] · N. Mendes[1] · C. Calderini[3] · P. X. Candeias[2] · M. Rossi[4] · P. B. Lourenço[1]

N. Mendes
nunomendes@civil.uminho.pt

C. Calderini
chiara.calderini@unige.it

P. X. Candeias
pcandeias@lnec.pt
http://www.lnec.pt

M. Rossi
michela.rossi@ec.europa.eu

P. B. Lourenço
pbl@civil.uminho.pt

[1] Institute for Sustainability and Innovation in Structural Engineering (ISISE), University of Minho, Campus de Azurém, 4800-058 Guimarães, Portugal

[2] Earthquake Engineering and Structural Dynamics Unit (NESDE), Department of Structures, Structures Department, National Laboratory for Civil Engineering (LNEC), Avenida Do Brasil, 101, 1700-066 Lisbon, Portugal

[3] Department of Civil, Chemical and Environmental Engineering (DICCA), University of Genoa, Via Montallegro 1, 16145 Genoa, Italy

[4] Joint Research Centre (JRC), Safety and Security of Buildings Unit (E.4), European Commission, Via E. Fermi 2749, 21027 Ispra, Italy